AD-A045 905 SYRACUSE UNIV N Y DEPT OF CHEMICAL ENGINEERING AND --ETC F/G 20/11
ELASTIC-PLASTIC DEFORMATION IN CRACKED SOLIDS AND DUCTILE FRACT--ETC(U)
SEP 77 H W LIU, W HU, S KUO DAHC04-74-G-0165
UNCLASSIFIED MTS-HWL-1611-FR-977 ARO-11961.5-E NL

1 OF 1
AD A045905

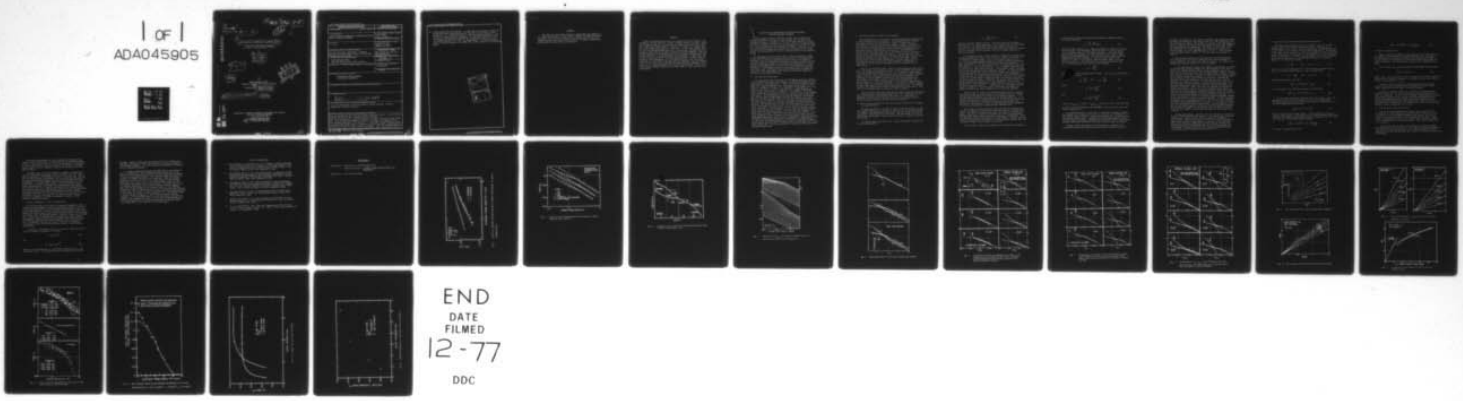

END
DATE FILMED
12-77
DDC

(18) ARO (19) 11961.5-E

(12)

(9) FINAL REPORT
1 Jul 74 - 30 June 77

(6) ELASTIC-PLASTIC DEFORMATION IN CRACKED SOLIDS AND DUCTILE FRACTURE CRITERION

by

(10) H. W. Liu
Wan-liang Hu
Sheng-yi Kuo

(11) Sep 77

(12) 39p.

for

ARMY RESEARCH OFFICE
Research Triangle Park, North Carolina

(15) Contract No. DAHC04-74-G-0165
DAA629-76-G-0290

(16) 1T161102BH57 (17) 06

Department of Chemical Engineering and Materials Science
OFFICE OF SPONSORED PROGRAMS
Syracuse University
Syracuse, New York 13210

(14) MTS-HWL-1611-FR-977

406 796

SECURITY CLASSIFICATION OF THIS PAGE *(When Data Entered)*

REPORT DOCUMENTATION PAGE		READ INSTRUCTIONS BEFORE COMPLETING FORM
1. REPORT NUMBER	2. GOVT ACCESSION NO.	3. RECIPIENT'S CATALOG NUMBER
4. TITLE *(and Subtitle)* ELASTIC-PLASTIC DEFORMATION IN CRACKED SOLIDS AND DUCTILE FRACTURE CRITERION		5. TYPE OF REPORT & PERIOD COVERED FINAL REPORT 7/1/74 - 6/30/77 6. PERFORMING ORG. REPORT NUMBER
7. AUTHOR(s) H. W. LIU		8. CONTRACT OR GRANT NUMBER(s) DAHC04-74-G-0165 DAA629-76-G-0290
9. PERFORMING ORGANIZATION NAME AND ADDRESS Syracuse University, Department of Chemical Engineering and Materials Science, 409 Link Hall Syracuse, New York, 13210		10. PROGRAM ELEMENT, PROJECT, TASK AREA & WORK UNIT NUMBERS R&D Project No. and Title 1T161102BH57-06 Mechanics and Aeronautics
11. CONTROLLING OFFICE NAME AND ADDRESS ARMY RESEARCH OFFICE Research Triangle Park, North Carolina		12. REPORT DATE September 1977 13. NUMBER OF PAGES
14. MONITORING AGENCY NAME & ADDRESS*(If different from Controlling Office)*		15. SECURITY CLASS. *(of this report)* Unclassified 15a. DECLASSIFICATION/DOWNGRADING SCHEDULE

16. DISTRIBUTION STATEMENT *(of this Report)*

APPROVED FOR PUBLIC RELEASE.
DISTRIBUTION UNLIMITED.

17. DISTRIBUTION STATEMENT *(of the abstract entered in Block 20, if different from Report)*

18. SUPPLEMENTARY NOTES

The findings in this report are not to be construed as an official Department of the Army position, unless so designated by other authorized documents.

19. KEY WORDS *(Continue on reverse side if necessary and identify by block number)*

Crack tip deformation, crack tip stresses, ductile fracture, fracture toughnesses of ductile material.

20. ABSTRACT *(Continue on reverse side if necessary and identify by block number)*

Crack tip deformation and crack tip stresses have been studied. The information obtained thus far is used to analyze ductile fractures.
Crack tip deformation and crack tip stresses are highly affected by plate thickness. When the necking parameter, $(K/\sigma_Y)^2/t$, is equal to or larger than 48, strip necking takes place at a crack tip. In this case, Dugdale model of crack tip opening displacement CTOD, is applicable; and CTOD as well as thickness contraction can be used to measure fracture toughness. When the necking parameter is 18, Dugdale model of crack opening displacement, COD, is applicable, but no

DD FORM 1 JAN 73 1473 EDITION OF 1 NOV 65 IS OBSOLETE

SECURITY CLASSIFICATION OF THIS PAGE *(When Data Entered)*

20. strip necking has been observed. In this case, the concept of crack tip stress and strain characterization by COD as well as by the far field parameters, i.e. the applied stress σ_∞ and the overall elongation Δ, can be used to measure fracture toughness. For the limiting case of a very thick plate, the ASTM E24 committee has recommended a value of 0.4 for the necking parameter for valid K_{IC} measurements. The precise demarcations of various regions to use CTOD, COD, σ_∞ and Δ have yet to be investigated.

FOREWARD

The author of this report gratefully acknowledges the support of U.S. Army Research Office, Grant Numbers, DAHC04-74-G-0165 and DAA-629-76-G-0290. The study was conducted at the George Sachs Fracture and Fatigue Research Laboratory of the Department of Cehmical Engineering and Materials Science, Syracuse University.

ABSTRACT

Crack tip deformation and crack tip stresses have been studied. The information obtained thus far is used to analyze ductile fractures. Crack tip deformation and crack tip stresses are highly affected by plate thickness. When the necking parameter, $(K/\sigma_Y)^2/t$, is equal to or larger than 48, strip necking takes place at a crack tip. In this case, Dugdale model of crack tip opening displacement CTOD, is applicable, and CTOD as well as thickness contraction can be used to measure fracture toughness. When the necking parameter is 18, Dugdale model of crack opening displacement, COD, is applicable, but no strip necking has been observed. In this case, the concept of crack tip stress and strain characterization by COD as well as by the far field parameters, i.e. the applied stress σ_∞ and the overall elongation Δ, can be used to measure fracture toughness. For the limiting case of a very thick plate, the ASTM E24 committee has recommended a value of 0.4 for the necking parameter for valid K_{IC} measurements. The precise demarcations of various regions to use CTOD, COD, σ_∞ and Δ have yet to be investigated.

ELASTIC-PLASTIC DEFORMATION IN CRACKED SOLIDS AND DUCTILE FRACTURE CRITERION

Linear elastic fracture mechanics has been very successful in dealing with brittle fractures of high strength and low and medium toughness materials. According to the conventional practice, a large specimen is required to measure the valid K_{IC} value of a tough material. For a very tough material, the required specimen size could be too large for a typical laboratory testing machine to handle. Therefore, a new fracture criterion consistent with the basic principles of the linear elastic fracture mechanics is needed to measure high fracture toughness values.

The development of the linear elastic fracture mechanics is based on the crack tip elastic stress and strain fields. A thorough understanding of the crack tip deformation and the crack tip stresses in the case of general yielding is necessary to develop a reliable ductile fracture theory. A program on "elastic-plastic deformation in cracked solids and ductile fracture criterion" has been conducted at Syracuse University. Considerable progress has been made during the past two and a half years. The major results obtained thus far are summarized as follows. The details have been reported in published papers and reports, see the publication list.

A. Crack Opening Displacement

The applicability and limitations of the Dugdale model are examined. Crack opening displacements are measured, and the measurements are compared with the calculated values. Figure 1 illustrates the COD measurements for a 2024-0 aluminum alloy. The tensile yield strength of the alloy is 53.8 MN/m^2 (7.8 ksi). The thicknesses of Specimen 1 and 2 are 0.041 cm and 0.625 cm (0.016 in. and 0.25 in.). Both specimens are loaded to the same K-value, 4.53 $MN/m^{3/2}$ (4.13 $ksi\sqrt{in}$). The dashed line represents the elastic calculation. The solid line is the Dugdale calculation. The measurements of the thin specimen agree exceedingly well with the plane stress Dugdale calculation; whereas, the measurements of the thick specimen agree well with the elastic calculation. The values of the quantity, $(K/\sigma_Y)^2/t$, for these two specimens are 17.5 and 1.12, where t and σ_Y are specimen thickness and tensile yielding strength. The quantity gives plastic zone size relative to plate thickness. This quantity is also an index of the deviation from the plane strain condition. The measurements clearly indicate that when a specimen is thin and the size of plastic zone is large, the COD measurements agree well with the Dugdale model. For this case, the condition of plane stress prevails. When the plastic zone is small relative to the plate thickness, and the condition of plane strain prevails, the COD measurements agree well with the elastic calculation. The same observation has also been made using 2024-T3 and 2024-T351 aluminum alloys. It is clear that the COD measurements are affected by specimen thickness, and it can be concluded that the Dugdale model is applicable only to the plane stress case. It is not suitable for plane strain analyses without suitable modifications.

B. The Characteristics of Near Tip Deformation

The strains near the crack tips of a double-edge-notched specimen made of 2024-0 aluminum alloy are measured. The measurements are compared with elastic-plastic FEM calculations. Figure 2 illustrates the measurements at various load levels in general yielding. The dashed lines represent the plane stress elastic-plastic FEM calculations. Near the crack tip, the measured strains are less than those obtained from the plane stress, elastic-plastic calculations. The difference is cuased by the stiffening effect due to the triaxial state of stress in the interior of the plate near the crack tip. In the interior of the plate, because that the hydrostatic tensile stress is high, and that the deviatoric stresses are low relative to those in the state of plane stress, there is less plastic deformation. In other words, close to the crack tip in the interior of a thick specimen, the material is "stiffened", and the state of deformation tends to approach that of plane strain.

Next to the "stiffened" zone, there is a characteristic plane stress zone. The slopes of the measured curves and the calculated curves agreed well with the HRR singularity, $1/(1 + N)$. If a sample is large enough, it is conceivable that a characteristic crack tip elastic field may exist. Further away, the stresses and strains are no longer dominated by the crack tip. They are largely controlled by the overall geometry and the loading of the sample. Figure 3 illustrates schematically the various regions in a very large specimen. One or more of these regions may not appear in a particular specimen. If a specimen is small, general yielding takes place, and the elastic region may not exist. In a bending specimen, the characteristic plane stress region may be very small. The size of the stiffened zone is affected by plate thickness.

Both the COD and the strain measurements indicate that the deformation in a cracked sample is three-dimensional in nature. Both plane strain and plane stress are idealized limiting cases. It is important to establish the conditions of validity for these two idealized cases in order to develop a reliable ductile fracture criterion.

C. Direct Characterization of Crack Tip Stresses and Strains for Samples in General Yielding

The important result of the linear elastic fracture mechanics is that the fracture toughness of a material is invariant to the planar geometry of a sample. The derivation of the brittle fracture theory based on the principle of energy balance is well known. The same result can also be derived from the concept of direct characterization of crack tip stresses and strains.

In a small region near the tip of a crack, the elastic stresses are given by the equation:

$$\sigma_{ij} = \frac{K}{\sqrt{2\pi r}} f_{ij}(\theta) \quad , \qquad (1)$$

where K is stress intensity factor. Away from the crack tip region, Equation (1) is no longer applicable. Let us define the crack tip region by a boundary, r_e, within which the elastic stresses are given by Equation (1). The characterization of the crack tip stresses and strains by K in an elastic solid is obvious, and not of primary interest to ductile fractures.

If a specimen is made of metal, plastic deformation does take place within the plastic zone, r_p, at the crack tip. Within r_p, Equation (1) is certainly no longer valid. If r_p is much smaller than r_e, i.e., $r_p << r_e$, the stress relaxation within r_p caused by plastic deformation will have negligible effects on the stresses along the boundary r_e. In other words, if $r_p << r_e$, the stresses on r_e are essentially those given by Equation (1). This condition of $r_p << r_e$ is commonly referred to as the condition of small scale yielding. Let us examine several specimens made of the same material but of different geometry. If they are loaded to the same K-value, and if the condition of small scale yielding is satisfied by all of the specimens, the stresses on the boundaries, r_e's, of the same size and shape of these samples, are the same. One may look at the r_e's as free bodies of identical shape and identical size with identical boundary stresses. Therefore, the stresses and strains within the r_p's must be the same for all of the specimens. If one of the samples fails, it is reasonable to expect that the others will fail too. In this way, one reaches the conclusion; K_c is invariant to planar geometric variation. Since the crack tip stresses and strains are highly affected by the plate thickness, K_c is thickness dependent.

The fact that the value of K characterizes the crack tip stresses and strains within r_p is sufficient for concluding that K_c is constant, provided that the condition of small scale yielding is obeyed. It is not necessary to know the exact stresses and strains within r_p. r_e is linearly proportional to the specimen size. One can always satisfy the condition of small scale yielding by increasing the specimen size. Indeed, this was found to be true, and the well known size requirement for valid K_{Ic} measurements was established (ASTM STP 410).

The concept of direct characterization of crack tip stresses and strains is examined for plane stress case where general yielding takes place. The crack tip stresses and strains in small scale yielding and general yielding are calculated with FEM, and a direct correspondence between small scale yielding and general yielding is established. Thus, the crack tip stresses and strains of a small sample in general yielding can be characterized by the K-value of a corresponding specimen where the condition of small scale yielding is satisfied.

For the case of small scale yielding, the calculations are made for

a semi-circular region with boundary displacement conditions given by the elastic solution:

$$u_i = \frac{K_I}{E} \sqrt{\frac{2r}{\pi}}\, h_i(\theta) \quad , \tag{2}$$

where $h_i(\theta)$ are functions of θ. FEM calculations are made for the state of plane stress. The calculated effective stress, $\tilde{\sigma}$, and the strain, ε_{yy}, at various levels of K are shown in Figure 4. The lines within plastic zones are parallel, and their slopes are very close to those given by the HRR singularities. The same results are shown in the non-dimensionalized plots of Figure 5. The sum of the slopes of the curves of $\tilde{\varepsilon}_p$ and $\tilde{\sigma}$, in the plastic region is nearly unity, as is the sum for ε_{yy} and σ_{yy}. But the sum for ε_{xx} and σ_{xx} is much less than one. The plastic zone size is given by the equation:

$$r_p = \alpha \left(\frac{K_I}{\sigma_Y}\right)^2 \tag{3}$$

and α = 0.24 for the aluminum alloy treated. ε_{yy} and σ_{yy} in the plastic zone can be written as

$$\varepsilon_{yy} = \frac{K_\varepsilon}{r^m} \quad \text{and} \quad \sigma_{yy} = \frac{K_\sigma}{r^{m'}} \tag{4}$$

where

$$K_\varepsilon = \frac{\varepsilon_Y}{\beta}\, \alpha^m \left(\frac{K_I}{\sigma_Y}\right)^{2m} \tag{5}$$

and

$$K_\sigma = \frac{\sigma_Y}{\beta'}\, \alpha^{m'} \left(\frac{K_I}{\sigma_Y}\right)^{2m'} \tag{6}$$

$(\varepsilon_Y/\beta) = \varepsilon_{yy(r=r_p)}$, $(\sigma_Y/\beta') = \sigma_{yy(r=r_p)}$, and β and β' are 1.405 and 0.983. K_ε and K_σ can be considered as the strengths of the crack tip strain and stress singularities.

As discussed earlier, in the case of a specimen in general yielding, the material in the region very close to a crack tip is "stiffened" by the triaxial state of stress. Beyond the stiffened zone, a characteristic plane stress region exists. Therefore for the specimen geometry chosen for this study, the direct correspondence between the cases of small scale yielding and general yielding in the state of plane stress is examined.

Figure 6 shows the results of the plane stress calculation of a double-edge-notched (DEN) specimen made of batch C aluminum in general

yielding. In addition to the crack line results, the y-direction stress and strain distributions along radial lines, 45°, 60° and 90° away from the crack line are shown. The results are plotted in the same manner as those in Figure 5, and the corresponding plots for small scale yielding are also presented for comparison. The values of r_p for these plots are obtained by the linear extrapolation of effective stress, $\bar{\sigma}$, to yield strength, σ_Y, in a logarithmic plot of $\bar{\sigma}$ vs. r. The calculated $\bar{\sigma}$ and effective plastic strain, $\bar{\varepsilon}^p$, are also shown and compared in Figure 7.

Plane stress calculation is also made for a single-edge-notched (SEN) specimen made of the same material loaded into the region of general yielding. The results are shown in Figure 8. The plane stress characteristic region (region II) is clearly shown.

In the characteristic plane stress region, the excellent correlation between both the general yielding cases (DEN and SEN) and the case of small scale yielding indicates that a single parameter, such as r_p, is sufficient to characterize the crack tip stresses and strains. Furthermore, the near tip stress or strain of a small sample in general yielding can be used to obtain the equivalent K_I value of a large specimen where the condition of small scale yielding is satisfied. Consider two specimens of the same thickness, one large and one small. Both are loaded to the level such that at a certain distance from crack tip, r, the y-direction stress or strain is the same for both specimens. The large specimen is wide enough such that the condition of small scale yielding is retained. Hence, the crack tip stresses and strains are characterized by the value of the stress intensity factor, which is given by the elastic solution; whereas the second specimen is so small that the state of deformation is general yielding. Since the crack tip strain and stress distributions are the same in both specimens, it is fair to say that the K_I value of the small specimen in general yielding is the same as the K_I value of the large specimen. In this connection, Equations (4,5,6) are applicable even in the case of general yielding as long as the corresponding pair of ε_{yy} and r, or σ_{yy} and r are taken from the characteristic plane stress region. By this approach, one is able to use a small sample to evaluate a very high fracture toughness. The equivalent K_I values for the empirical data in Figure 2 are 38.5, 29.8, and 23.3 ksi$\sqrt{\text{in}}$. The tensile yield stress of this material is 7.26 ksi.

As discussed earlier, near the crack tip, the state of stress and strain is three-dimensional in nature. It is neither plane strain nor plane stress. However, if the stiffened region is embedded in a characteristic plane stress region, if the size of the characteristic plane stress region is large relative to the size of the stiffened zone, and if the plate thicknesses are the same, the stresses and strains within the stiffened zone must be the same even though they are unknown. Therefore, the crack tip stresses and strains can be characterized by the equivalent plane stress K or J.

D. Near Tip Strain and Stress and Far Field Parameters

In Figure 9 the normalized crack line strain, $\varepsilon_{yy}/\varepsilon_Y$, of the DEN specimen calculated at various distances from the crack tip, r, is plotted against $\Delta/W\varepsilon_Y$, where Δ is the elongation of the DEN specimen over a gage length of seven inches, and W is the specimen width. The results of the plane stress calculation, which are represented by the solid lines, agree well with the limited number of measurements, i.e., the triangular points in the figure. A similar relation between the crack line stress, σ_{yy} at various distances, r, and the applied stress σ_∞ is shown in Figure 10. In the linear regions,

$$\varepsilon_{yy} = \gamma\frac{\Delta}{W} \quad , \qquad \text{and} \qquad \sigma_{yy} = \gamma' \sigma_\infty \quad , \tag{7}$$

where γ and γ' are functions of r/W. These results also imply that K_ε and K_σ are linearly proportional to Δ and σ_∞ respectively

$$K_\varepsilon = \Gamma\left(\frac{\Delta}{W}\right) \qquad \text{and} \qquad K_\sigma = \Gamma'\sigma_\infty \tag{8}$$

Combining Equations (5) and (8),

$$K_I^{2m}\left[(\varepsilon_Y \alpha^m/\beta)\sigma_Y^{-2m}\right] = \Gamma\left(\frac{\Delta}{W}\right) \quad . \tag{9}$$

In a like manner, the following relation can be derived,

$$K_I^{2m'}\left[(\sigma_Y \alpha^{m'}/\beta')\sigma_Y^{-2m'}\right] = \Gamma' \sigma_\infty \tag{10}$$

If the linear relations of Equation (8) do not exist, Γ and Γ' in Equations (9) and (10) are functions of (Δ/W) and σ_∞ respectively. Multiplying Equations (9) and (10) and recalling the relation $m+m' \simeq 1$, the final approximated form becomes

$$K_I^2/E = [\beta\beta'\Gamma\Gamma'/\alpha]\,\frac{\sigma_\infty\Delta}{W} \tag{11}$$

K_I^2/E is J in the case of plane stress. If the product of $\varepsilon_{yy}\,\sigma_{yy}$ is linearly proportional to the product $\Delta\sigma_\infty$ for a given geometry and a given material, the quantity in the square bracket of Equation (11), $\beta\beta'\Gamma\Gamma'/\alpha$, is a constant. For the DEN specimen treated,

$$K_I^2/E = 3.37\,\frac{\sigma_\infty\Delta}{W} = 16.1\,\left(\frac{\sigma_\infty}{\sigma_Y}\right)\left(\frac{\Delta}{W\varepsilon_Y}\right) \tag{12}$$

for batch C aluminum alloy, and

$$K_I^2/E = 3.67 \frac{\sigma_\infty \Delta}{W} = 34.5 \left(\frac{\sigma_\infty}{\sigma_Y}\right)\left(\frac{\Delta}{W\varepsilon_Y}\right) \qquad (13)$$

for batch B aluminum alloy.

Figure 11 plots the product of σ_{yy}/σ_Y and $\varepsilon_{yy}/\varepsilon_Y$ as a function of the product of its associated far field parameters σ_∞/σ_Y and $\Delta/W\varepsilon_Y$. It is interesting to note that the deviation from linearity in Figure 11 is not as severe as in Figures 9 and 10 where stresses and strains are plotted separately. The stresses and strains tend to compensate each other.

If the product $\varepsilon_{yy}\ \sigma_{yy}$ is not linearly proportional to the product $\Delta\sigma_\infty$,

$$K_I^2/E = (\beta\beta'\Gamma\Gamma'/\alpha) \qquad (14)$$

where Γ and Γ' are functions of Δ and σ_∞ respectively, and the functional relation can be derived by numerical calculations such as those shown in Figure 11 with $(K_\varepsilon K_\sigma/r) = \varepsilon_{yy}\sigma_{yy}$.

Equations (11) and (14) relate the equivalent stress intensity factor to the overall elongation and the applied stress for a small sample loaded far into the region of general yielding.

The stress intensity factor, K_I, is plotted at various loading levels in Figure 12. The elastic solutions are also included in the plots for comparison. In the region of general yielding where the linear relationship between the near tip and far field parameters hold, the curves are approximated by the dashed lines given by Equation (11). When the linearity breaks down, the equivalent K_I values can still be obtained by the correlations of the characteristic near tip stresses and strains as given by Equations (5) and (6).

E. Near Tip Strain Fracture Criterion

Near tip strain measurements were made at the onset of surface crack growth in three tough and ductile materials: HY-80 steel, and two batches of a fully annealed aluminum alloy (batch B and batch C). Fatigue pre-cracked specimens were tested under tensile load. Three types of specimens were tested: WOL, SEN and DEN. All the specimens of each material were of the same thickness. Their widths ranged from 2 to 8 inches.

At the first sign of surface crack growth, the near tip strains were measured with the moire method. The results are shown in Figure 13. The cross in the second figure for batch C 2024-0 aluminum alloy was measured with a small strain gage, which agreed well with the moire strain measurements.

The strain measurements for each of these three materials fall within a narrow band in spite of the differences in specimen geometry and size. This indicates that at the first appearance of crack growth on the specimen surface, near tip strain is not affected by specimen geometry and the type of loading as long as the specimens are of the same thickness.

A careful study of the data presented in Figure 13 reveals that the three dimensional stiffening effects are shown in all the three types of specimen at the immediate vicinity of the crack tip. For the WOL and SEN specimens, the bending effect is so dominant that there is no plane stress deformed region that can be detected from the strain measurements. A longer ligament width should be considered for this observation. For the DEN type specimen, the characteristic plane stress deformed region is noticeable at approximately one thickness away from the crack tip. Based on the strains in the characteristic plane stress region of the DEN specimen, the K_c value of this particular material (batch B aluminum alloy) is estimated to be 69.1 ksi$\sqrt{\text{in}}$ according to Equation (5). The value of $(K_c/\sigma_Y)^2$ is close to 50 inches. According to the size requirement of the linear elastic fracture mechanics, a ligament of 10 feet is necessary to conduct a valid fracture toughness measurement.

F. Fracture Toughnesses of Thin and Tough Plates

Wells has proposed to use crack tip opening displacements, CTOD, to measure fracture toughness in the case of general yielding. The crack tip opening displacements and the thickness contractions of thin steel plates were measured. For thin and ductile plates, when the crack tip plastic zone size is much larger than the plate thickness, strip necking takes place, when the necking parameter, $(K/\sigma_Y)^2/t$, equals to or exceeds 48. In this case, the Dugdale model is applicable to the "opening displacements" between the upper and the lower crack surfaces as well as between the upper and the lower boundaries of the strip necking zone. Furthermore, the data in Figure 14 show that the opening displacements in the strip necking zone are equal to the thickness contractions.

According to the Dugdale model, K is related to CTOD; and CTOD is equal to thickness contraction. Therefore

$$K = (E\sigma_Y \Delta t)^{1/2} \tag{15}$$

and

$$K = (E\sigma_Y \, t_o \varepsilon_z)^{1/2} \tag{16}$$

where Δt is the contraction; t_o, the initial thickness; and ε_z, the contraction strain. The contractions can be measured from a broken

specimen. Figure 15 shows the measured R-curves of two HY-80 steel specimens, and Figure 16 shows the variation of fracture toughness, K_c, with specimen thickness. The curves show the characteristic decrease in K_c as thickness decreases.

In summary, significant progress has been made in the studies of crack tip deformation, and the knowledge obtained thus far is very useful to develop practical methods of fracture toughness measurements for ductile and tough materials. Crack tip deformation and crack tip stresses are highly affected by plate thickness. When the necking parameter, $(K/\sigma_Y)^2/t$, is equal to or larger than 48, strip necking takes place at a crack tip. In this case, Dugdale's model of crack tip opening displacement, CTOD, is applicable. Therefore CTOD as well as thickness contraction can be used to measure fracture toughness. When the necking parameter is 18, Dugdale's model of crack opening displacement, COD, is applicable, but no strip necking has been observed. In this case, the concept of crack tip stress and strain characterization by COD as well as by the far field parameters, i.e., the applied stress σ_∞ and the overall elongation Δ, can be used to measure fracture toughness. For the limiting case of a very thick plate, the ASTM E24 committee has recommended a value of 0.4 for the necking parameter for valid K_{IC} measurements. The precise demarcations of various regions to use CTOD, COD, σ_∞ and Δ have yet to be investigated.

LIST OF PUBLICATIONS

1. Wan-liang Hu, A. S. Kuo and H. W. Liu, "A Study on Crack Tip Deformation and Ductile Fracture," Proceedings of 12th Annual Meeting of the Society of Engineering Science, Austin, Texas, October (1975). Also as Technical Report, August 1975, submitted to ARO.

2. Wan-liang Hu and H. W. Liu, "Crack Tip Strains - A Comparison of FEM Calculations and Measurements," Ninth National Symposium on Fractured Mechanics, University of Pittsburgh, Pittsburgh, Pa. (1975). Also as Technical Report, April 1975, submitted to ARO.

3. Wan-liang Hu and H. W. Liu, "Characterization of Crack Tip Stresses and Strains - Small Scale Yielding and General Yielding," Proceedings, 2nd. Int. Conf. on Mech. Behavior of Materials, Boston, Mass., August (1976). Also as Technical Report, May 1976, submitted to ARO.

4. Wan-liang Hu and H. W. Liu, "A Finite Element Study on Crack Tip Deformation," Dept. of Chem. Eng. and Materials Science, August 1976. Report submitted to ARO.

5. Albert S. Kuo and H. W. Liu, "An Experimental and FEM Study on Crack Opening Displacement," Proceedings of the Fourth Int. Conf. on Fracture, Waterloo, Canada, June (1977).

6. H. W. Liu and Albert S. Kuo, "Fracture Toughnesses of Thin and Tough Plates," Technical Report, August 1977. Dept. of Chem. Eng. and Materials Science, to be submitted to ARO.

PARTICIPANTS

Wan-liang Hu - completed Ph.D. program August 1976

Dissertation title: A FINITE ELEMENT STUDY ON CRACK TIP DEFORMATION.

Sheng-yi Kuo - Post Doctoral Fellow

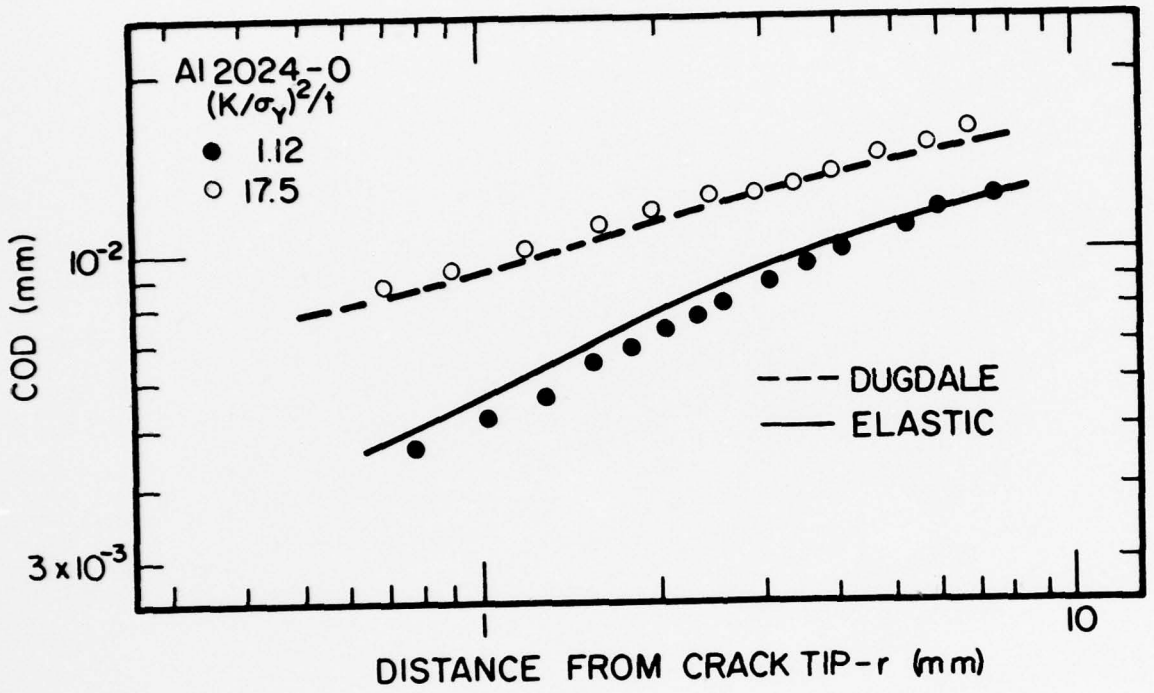

FIG. 1. EFFECT OF SPECIMEN THICKNESS ON CRACK OPENING DISPLACEMENT: Al 2024-O ALUMINUM ALLOY.

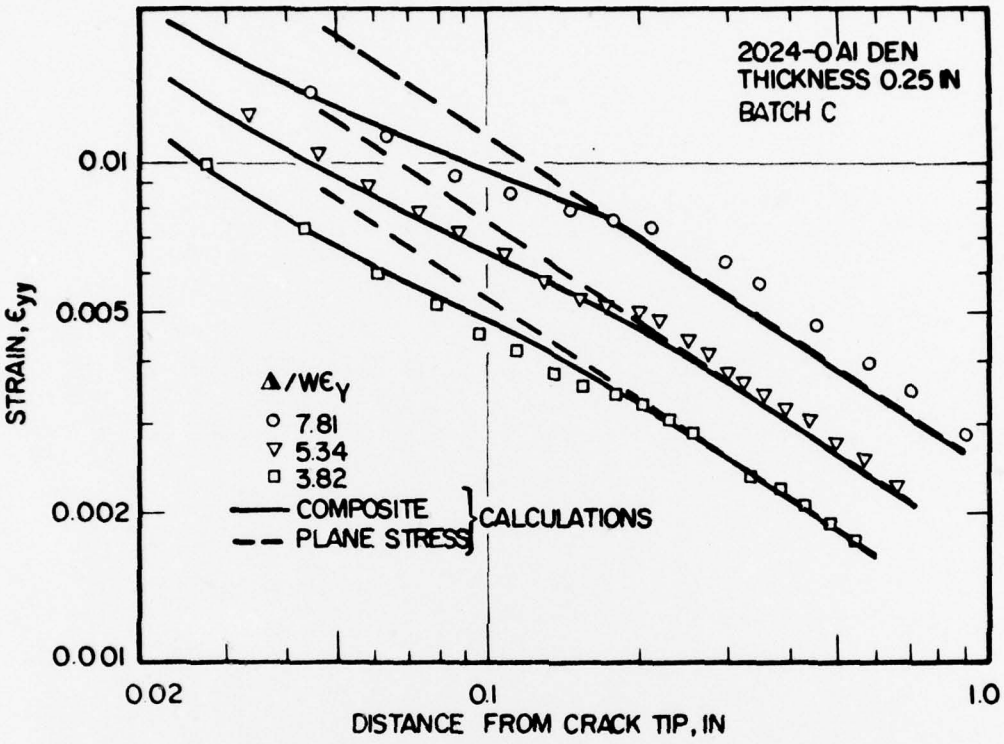

Fig. 2. Near tip strain measurements and calculations, 2024-0 aluminum alloy, batch C.

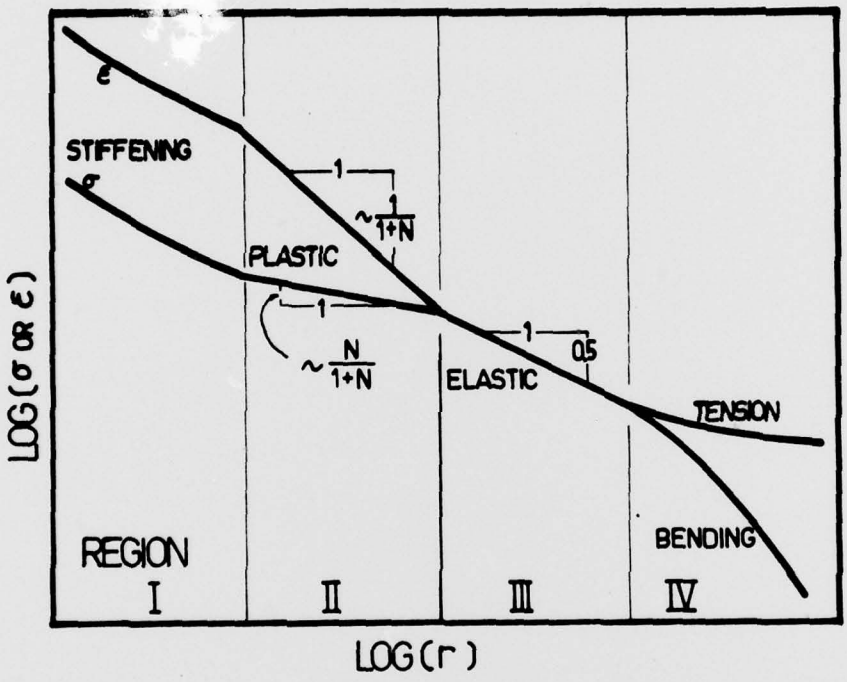

Fig. 3. Schematic plot of stress and strain distributions ahead a crack in logarithmic scale.

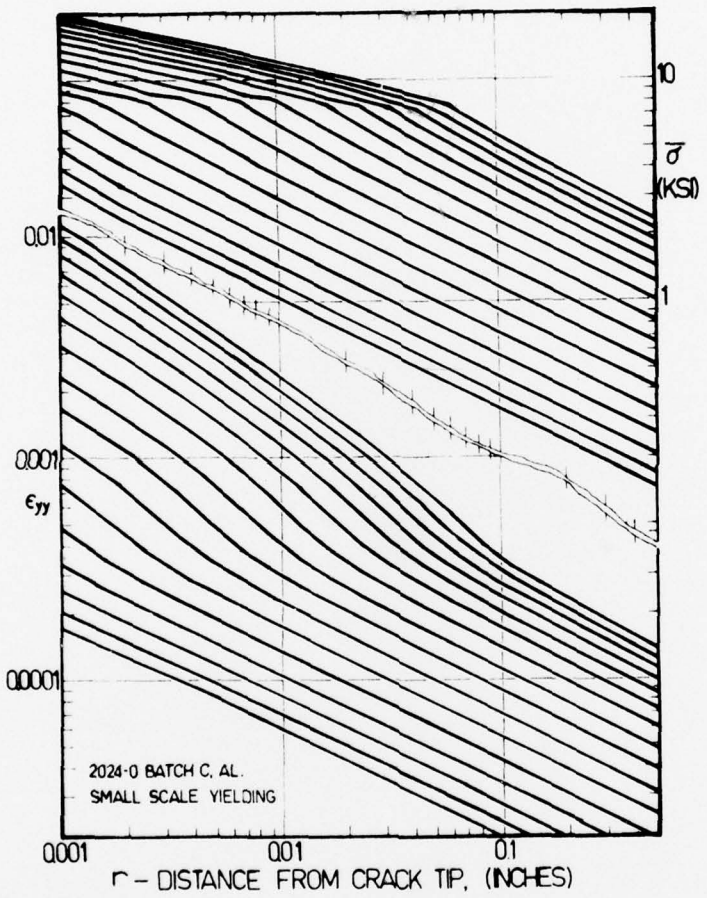

Fig. 4. Calculated $\bar{\sigma}$ and ε_{yy} for batch C aluminum along the crack line in small scale yielding case.

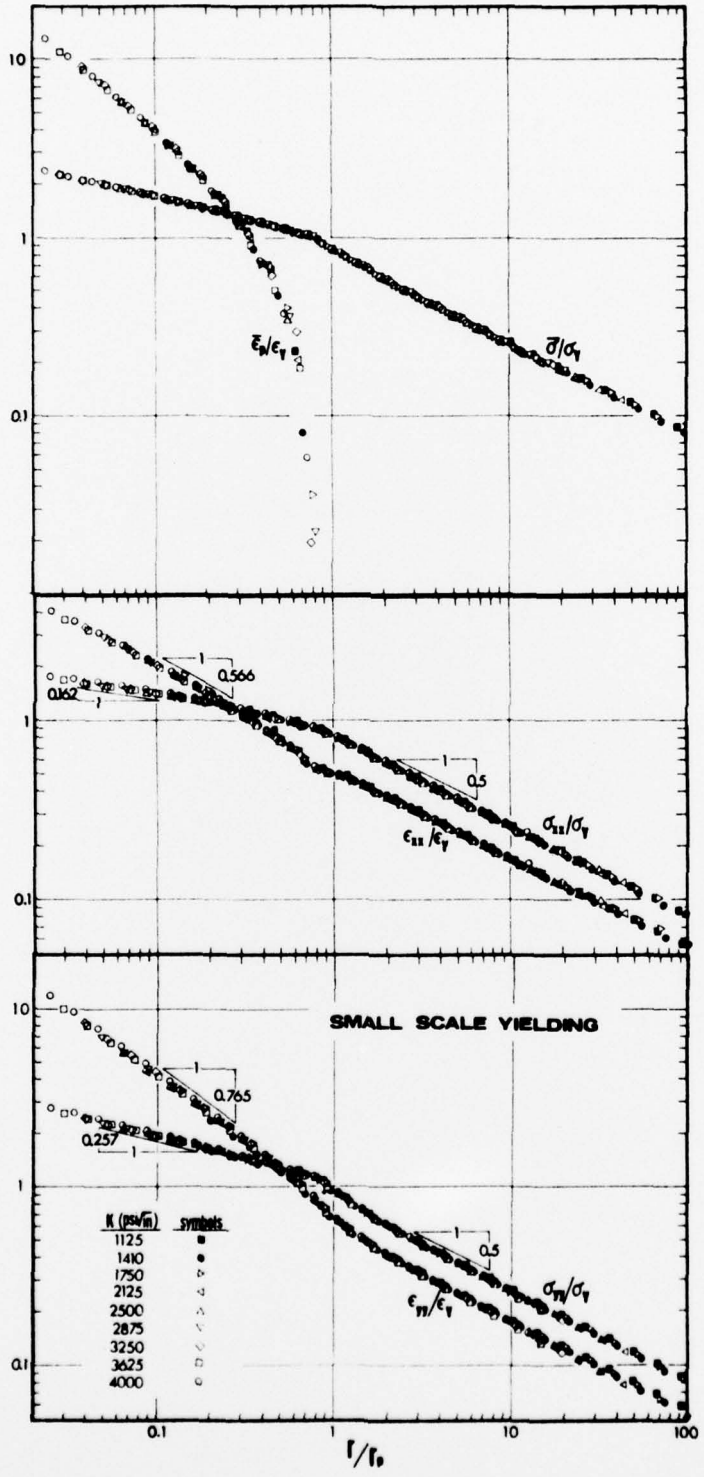

Fig. 5. Normalized plots of crack line stresses and strains.

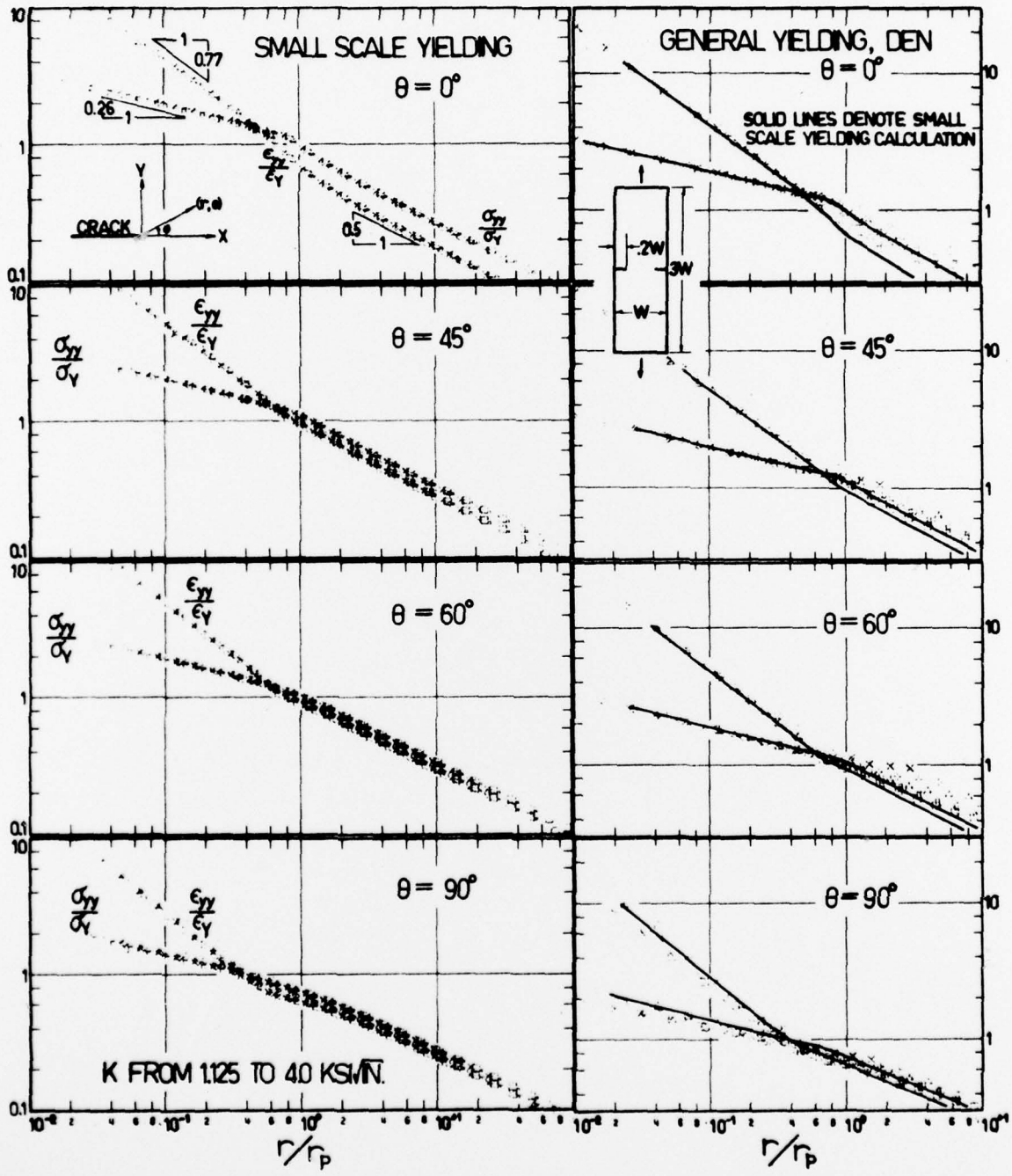

Fig. 6. Correlations of near tip stresses and strains in the loading direction between the small scale yielding and double-edge-notched specimen loaded into the region of general yielding.

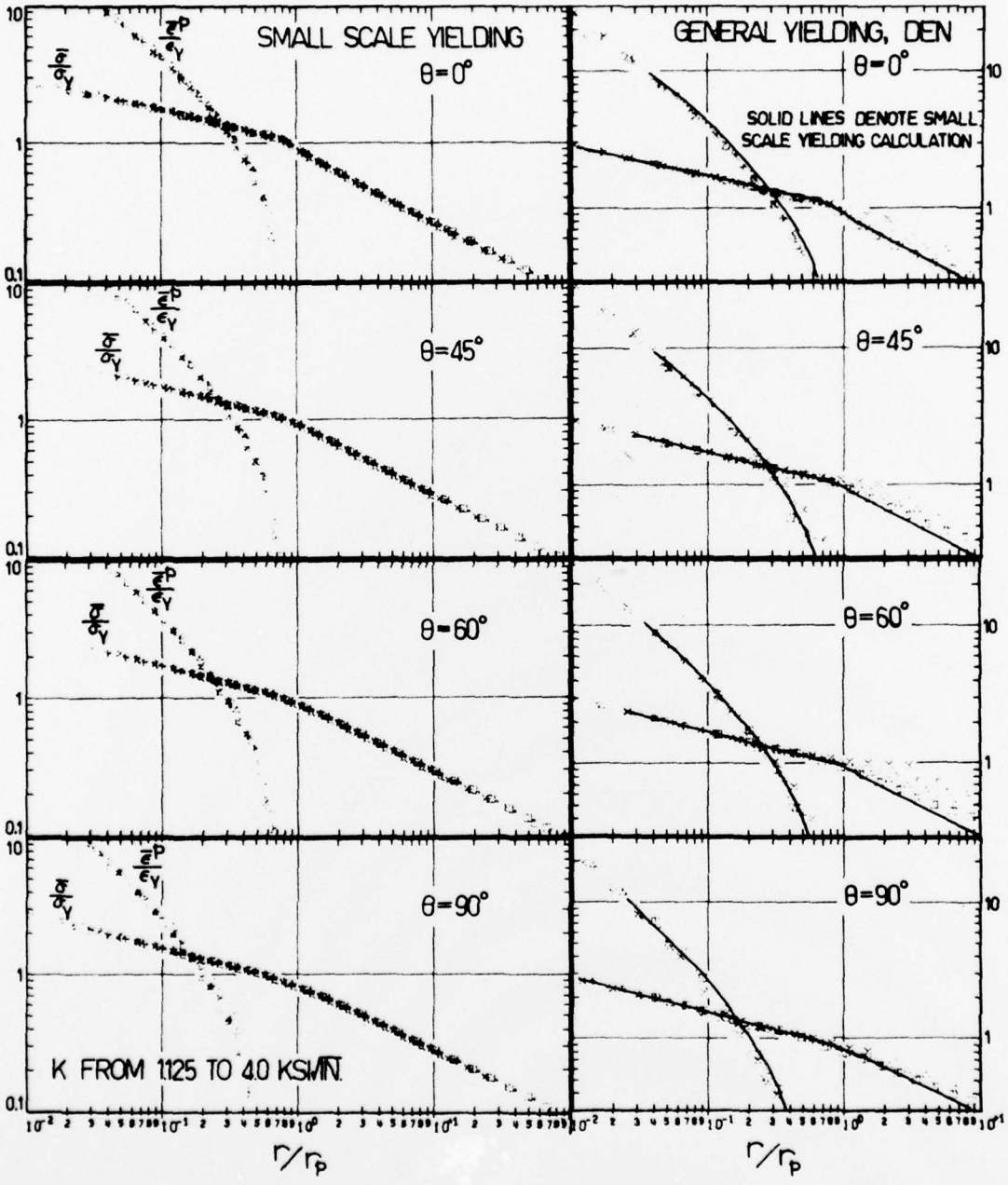

Fig. 7. Correlations of effective stress and effective plastic strain between the small scale yielding and double-edge-notched specimen loaded into the region of general yielding.

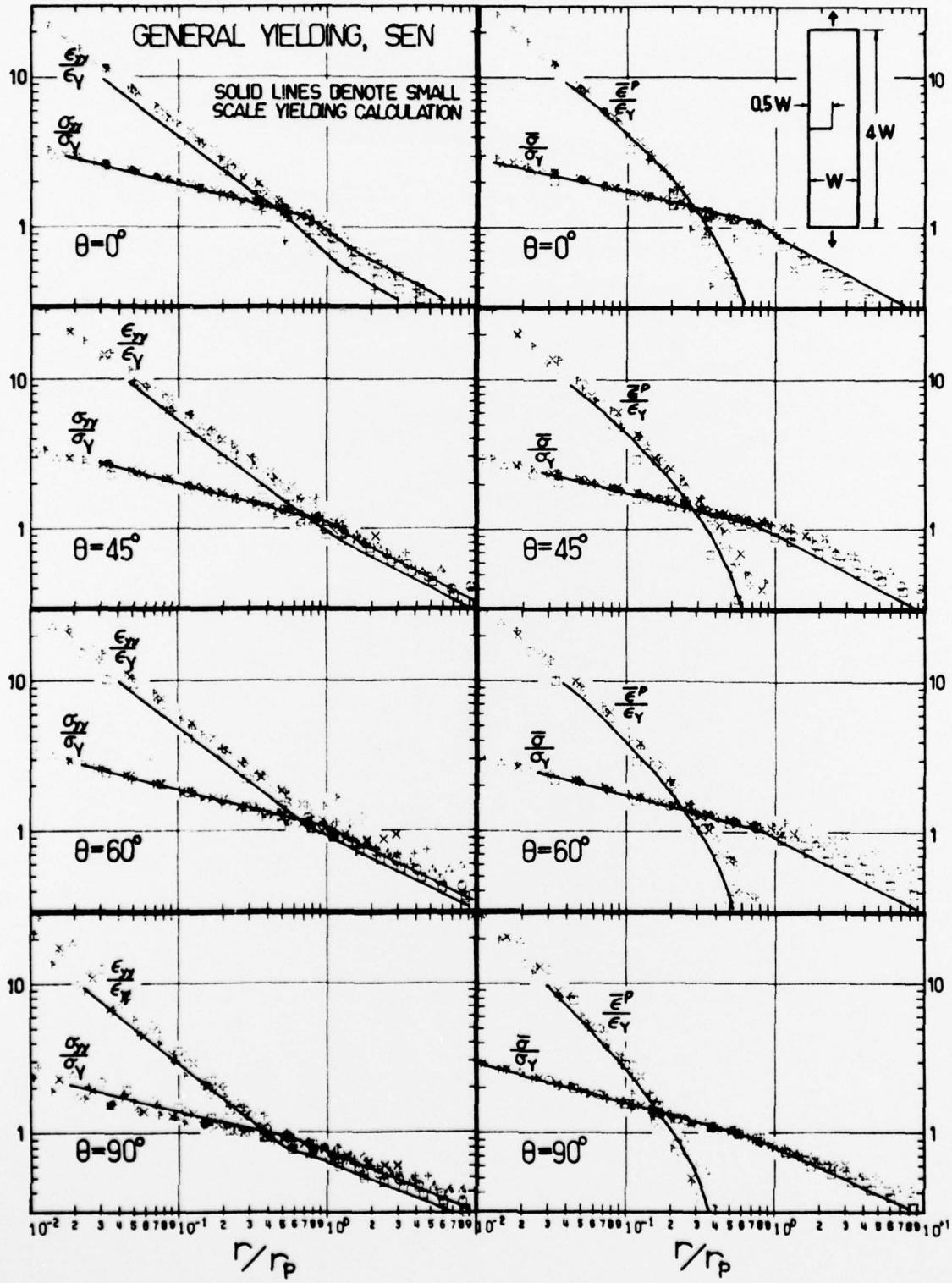

Fig. 8. Correlations of σ_{yy}, ε_{yy}, $\bar{\sigma}$ and $\bar{\varepsilon}^p$ between the small scale yielding and single-edge-notched specimen loaded into the region of general yielding.

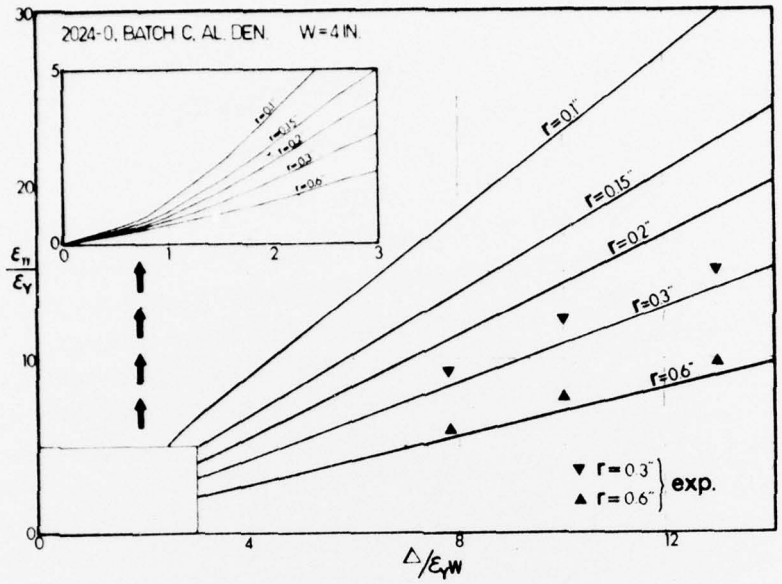

Fig. 9. The relation of near tip strain and gross elongation.

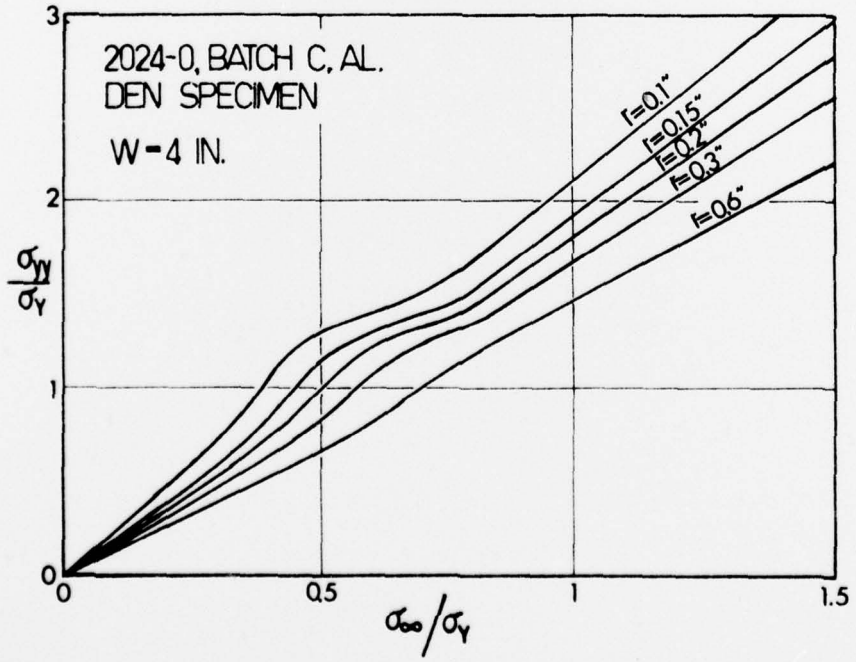

Fig. 10. The relation of near tip stress and applied stress.

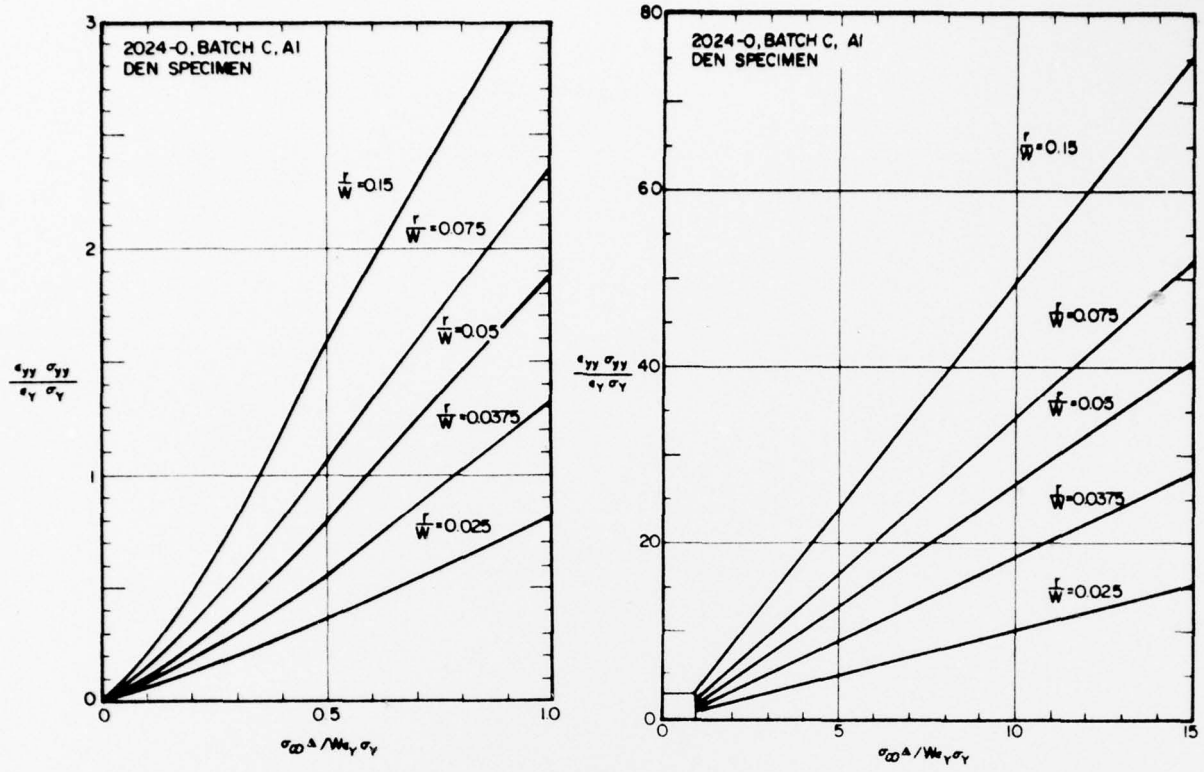

Fig. 11. Near field parameter, $\sigma_{yy}\varepsilon_{yy}/\sigma_Y\varepsilon_Y$ versus far field parameter, $\sigma_\infty\Delta/W\sigma_Y\varepsilon_Y$.

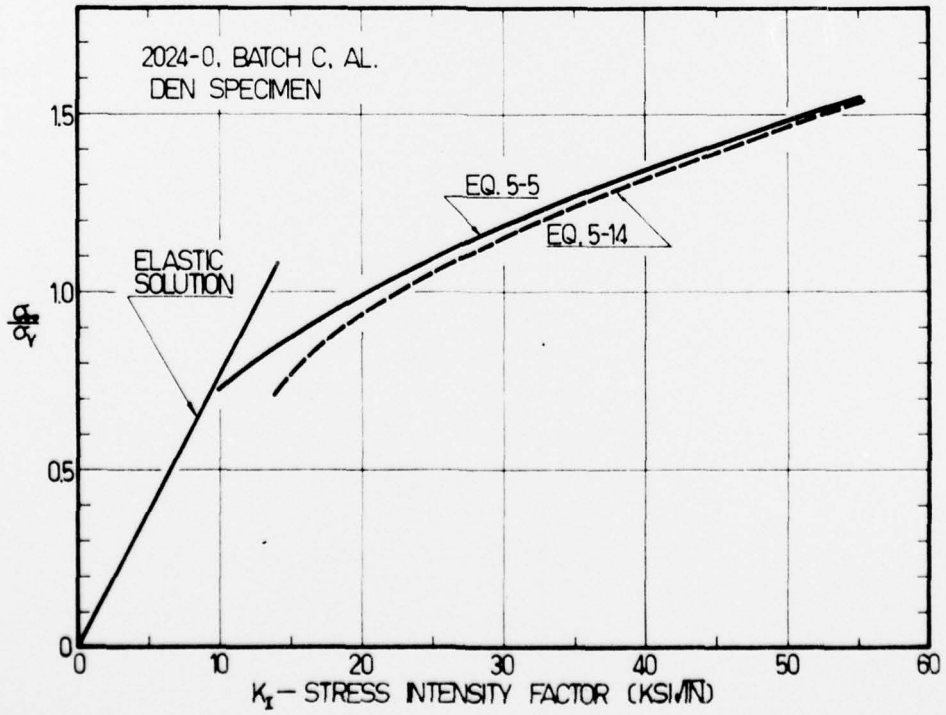

Fig. 12. Calculated stress intensity factor at various loading levels.

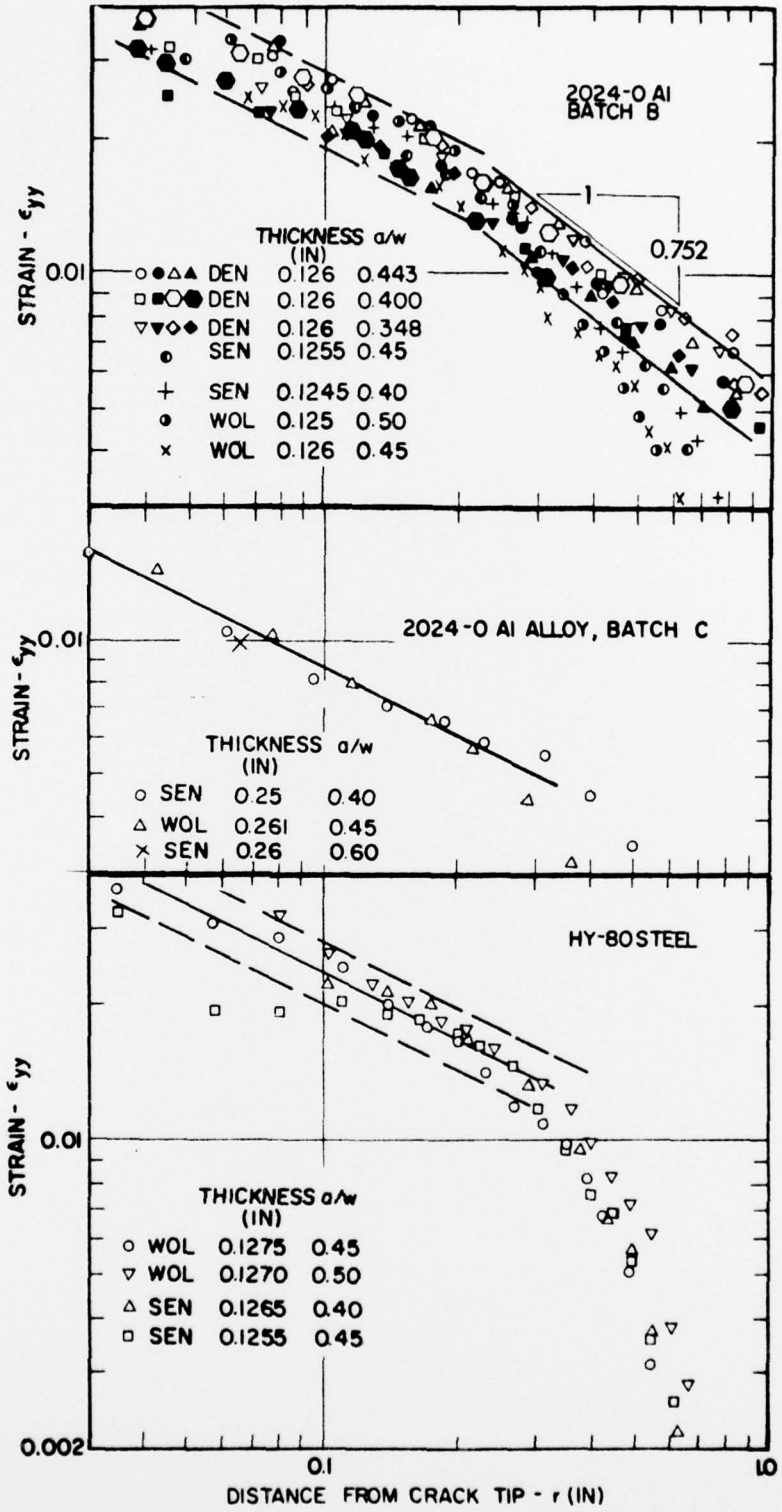

Fig. 13. Near tip strain measurements at the onset of slow crack growth on specimen surface.

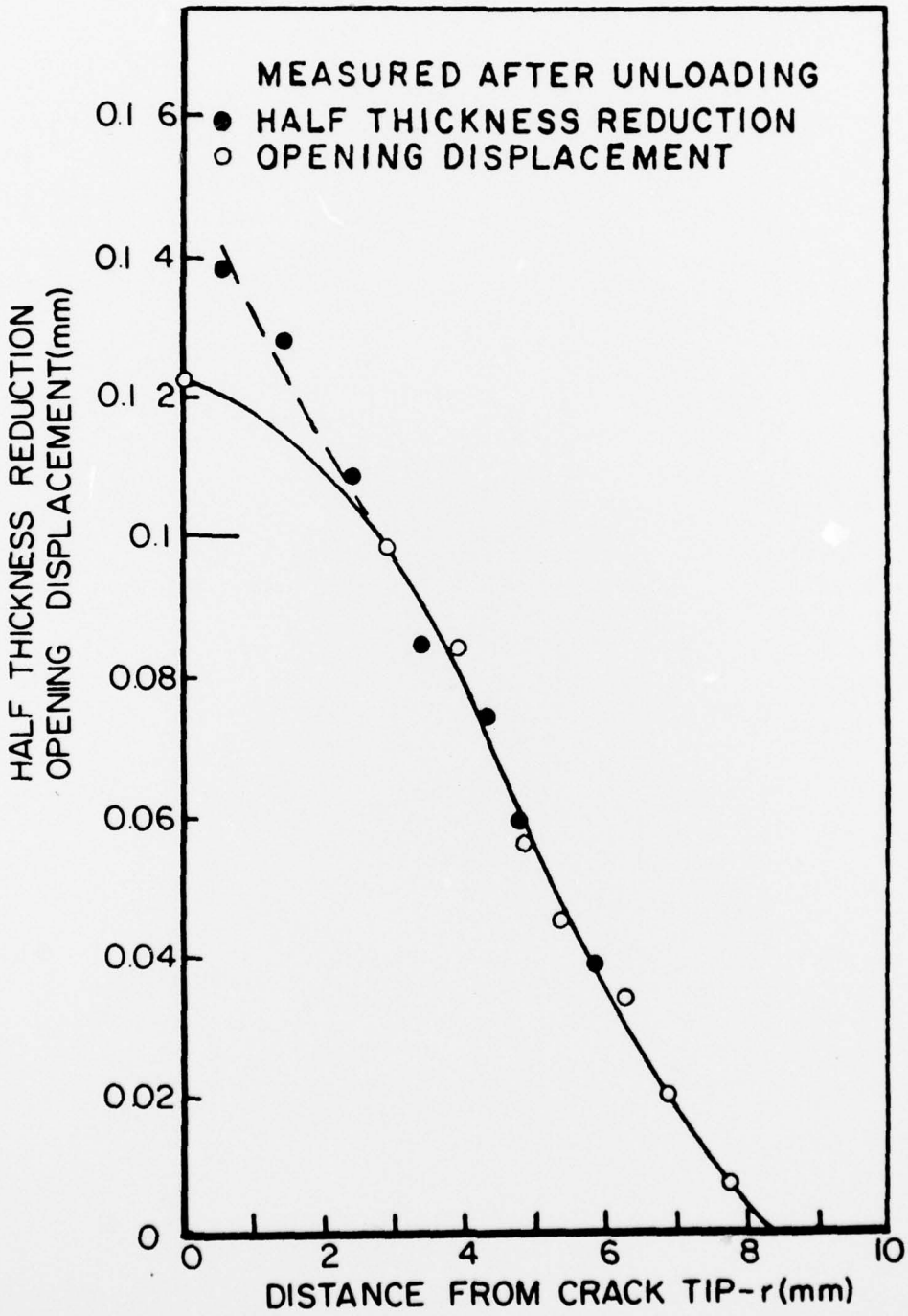

FIG. 14. HALF-THICKNESS REDUCTION AND OPENING DISPLACEMENT IN THE STRIP NECKING REGION OF A STEEL SPECIMEN: σ, 380 MN/m^2; σ_Y, 627 MN/m^2.

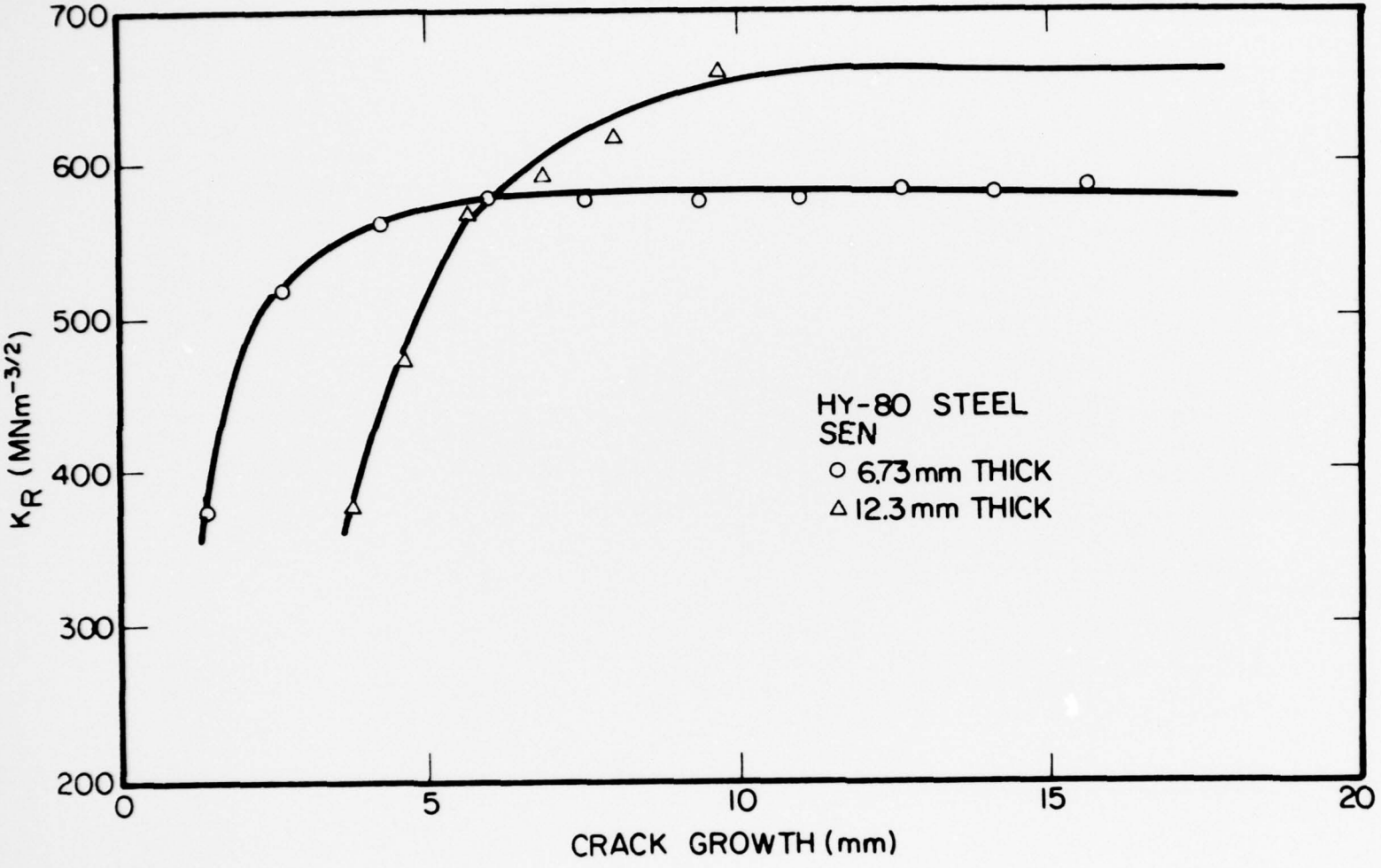

FIG. 15. R-CURVE FOR HY-80 STEEL SPECIMENS.

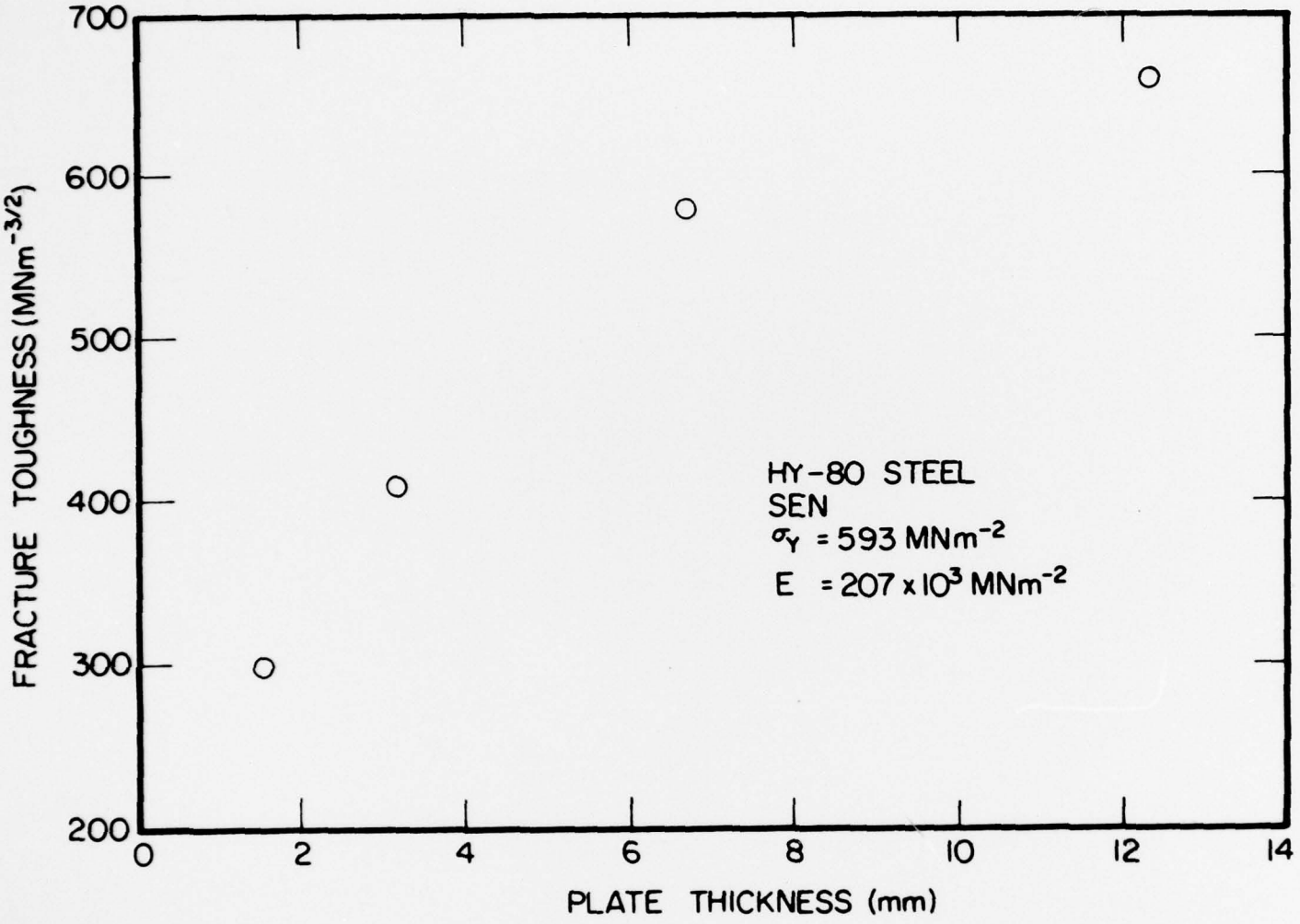

FIG. 16. FRACTURE TOUGHNESS AS A FUNCTION OF PLATE THICKNESS.